Mid-infrared Er:ZBLAN fiber laser reaching 3.68 μm wavelength

Zhipeng Qin (覃治鹏), Guoqiang Xie (谢国强)*, Jingui Ma (马金贵), Peng Yuan (袁 鹏), and Liejia Qian (钱列加)

Key Laboratory for Laser Plasmas (Ministry of Education), Collaborative Innovation Center of IFSA (CICIFSA), School of Physics and Astronomy, Shanghai Jiao Tong University, Shanghai 200240, China

**Corresponding author: xiegq@sjtu.edu.cn*

Received August 9, 2017; accepted September 8, 2017; posted online September 22, 2017

We report a continuous-wave Er:ZBLAN fiber laser with the operation wavelength reaching 3.68 μm. The mid-infrared Er:ZBLAN fiber laser is pumped with the dual-wavelength sources consisting of a commercial laser diode at 970 nm and a homemade Tm-doped fiber laser at 1973 nm. By increasing the launched pump power at 1973 nm, the laser wavelength can be switched from 3.52 to 3.68 μm. The maximum output power of 0.85 W is obtained with a slope efficiency of 25.14% with respect to the 1973 nm pump power. In the experiment, the laser emission at 3.68 μm is obtained with a significant power of 0.62 W, which is the longest emission wavelength in free-running Er:ZBLAN fiber lasers.

OCIS codes: 140.3070, 060.2390, 060.3510, 140.3480.
doi: 10.3788/COL201715.111402.

There is an increasing interest to mid-infrared (2–20 μm) coherent sources in the last decade due to the potential applications in spectroscopy, defense, and sensing for trace gas detection and greenhouse gases monitoring[1–4]. Moreover, significant progresses have been made with high-power mid-infrared coherent sources, such as optical parametric oscillators (OPOs), quantum cascade lasers (QCLs), and rare-earth-doped fiber lasers[5–7]. While OPOs are capable of emitting high output power and good beam quality, they have a complex setup and large volume. QCLs can cover a wide range of mid-infrared wavelengths, however, the output powers are limited below the watt level at the 3.5 μm band[6]. Fiber lasers possess the merits of high power, compactness, low cost, and good beam quality. Currently, fiber lasers become an important route to exploit high-power mid-infrared coherent sources.

So far, continuous-wave (CW) and pulsed laser sources at the 2.8 μm wavelength have been widely investigated based on Er-doped and Ho-doped fluoride glass fiber lasers[8–16]. However, limited by the available mid-infrared optical devices, fiber lasers beyond 3 μm are still underdeveloped. In the past decades, only a few groups carried out relevant research work, mainly focusing on CW Er-doped fluoride glass fiber lasers. The first CW laser at 3.45 μm was reported in 1991 at a 77 K temperature[17]. In the next year, a room-temperature Er:ZBLAN fiber laser was demonstrated at 3.48 μm with a low slope efficiency of 2.8%, pumped with a dicyanomethylene (DCM) dye laser at 655 nm[18]. For visible light pumping, the large quantum defect between mid-infrared and visible photons inherently results in low Stokes efficiency (~19%). However, this limit was broken, and Stokes efficiency was improved up to 56% with the advent of the dual-wavelength pumping (DWP) scheme, proposed by Henderson-Sapir *et al.* in 2013[19]. Accompanied by the advances in fluoride fiber fabrication and high-power pump source technologies, CW output power and optical-to-optical efficiency of a fluoride fiber laser are enhanced up to 260 mW and 16%, respectively[20]. Recently, 5.6 W of CW power was achieved by using fiber Bragg gratings (FBGs) instead of bulk reflectors operating at 3.55 μm[21]. In free-running Er-doped fluoride fiber lasers, multiple emission wavelengths were realized, and the longest emission wavelength reached 3.60 μm. Er-doped fluoride glass fibers usually have broad fluorescence spectra around 3.50 μm, originating from Starks splitting in the upper and lower energy levels[22]. The actual operation wavelength is influenced by the Er-doping concentration and glass composition[23]. For longer wavelength operation, a widely tunable Er:ZBLAN fiber laser was exploited[24]. However, the excess loss in the collimating optics resulted in a low output power of 50 mW. Up to now, there has been no report on a free-running Er-doped fluoride fiber laser beyond 3.60 μm wavelength.

In this Letter, we report a mid-infrared Er:ZBLAN fiber laser with the operation wavelength reaching 3.68 μm, which is the longest wavelength emitted from free-running Er:ZBLAN fiber lasers, to the best of our knowledge. The laser wavelength is switchable between 3.52 and 3.68 μm by varying the launched pump power of 1973 nm. The maximum output power of 0.85 W is obtained with a slope efficiency of 25.14% with respect to 1973 nm of pump power, and a significant power of 0.62 W is achieved at the 3.68 μm wavelength.

A simple linear cavity structure was adopted in the Er:ZBLAN fiber laser, as shown in Fig. 1. One end of the fiber was butted against an output coupler (OC). The OC had a transmission of 30% from 3300 to 4000 nm. Besides, it was anti-reflectively coated for pump wavelengths at 970 and 1973 nm. The other end of the

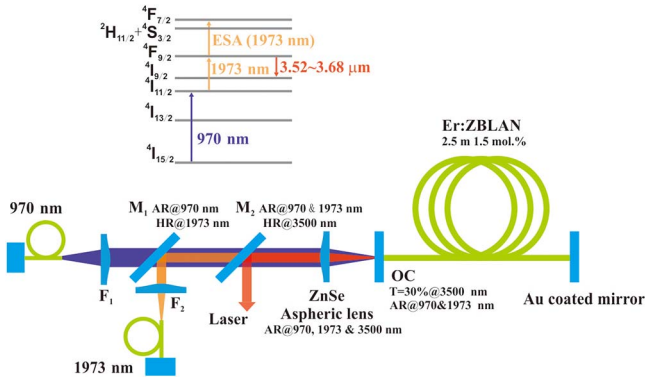

Fig. 1. Experimental setup of the dual-wavelength pumped Er:ZBLAN fiber laser. F_1, CaF_2 lens with $f = 18$ mm; F_2, ZnSe aspheric lens with $f = 12.7$ mm; ESA, excited state absorption. Inset: the energy level diagram of Er:ZBLAN.

fiber was butted against an Au coated mirror, which had high reflectivity for pump and laser wavelengths. For the Er-doped fluoride glass fibers, there is generally a difference in their fluorescence spectra induced by the different glass composition and Er-doping concentration. A gain peak redshift with the increase of Er-doping concentration was clearly shown in Ref. [23]. Compared with previous reports where 1.0 mol.% Er:ZBLAN fibers were usually used[18,20,21,24,25], here, we adopted a higher-doping Er:ZBLAN fiber (1.5 mol.%, Le Verre Fluoré) for longer wavelength operation. The gain fiber was 2.5 m long. The core diameter of the fiber was 16.5 μm with a numerical aperture (NA) of 0.15. The first cladding had a diameter of 260 μm with two parallel flats separated by 240 μm. The second cladding was a low-index fluoroacrylate polymer with a diameter of 290 μm. The DWP scheme in the Er:ZBLAN fiber laser could significantly increase the efficiency compared with visible light pumping. Here, the DWP scheme was adopted in our experiment (Inset of Fig. 1), which consisted of a commercial laser diode (LD) at 970 nm and a homemade Tm-doped fiber laser at 1973 nm. Since the excited state of $^4I_{11/2}$ has a long lifetime, a mass of electrons can populate here and form the so-called "virtual ground state" under the pumping of the LD at 970 nm. Then, these electrons cycle in the closed loop formed by the "virtual ground state", the upper laser level, and the lower laser levels, involving population inversion, laser emission, and multi-phonon decay. Once the electrons escape from the closed loop, they will be re-excited back to the "virtual ground state" by pumping at 970 nm. The coupling fiber of the LD at 970 nm had an NA of 0.2 and a core diameter of 105 μm. The coupling efficiency of the Er:ZBLAN fiber was measured to be 89% for pump light at 970 nm, and the fiber had an absorption of about 0.68 dB/m for cladding pumping at 970 nm. The pump light of 1973 nm was generated from a Tm-doped dual-cladding single-mode fiber (10/130 μm, 0.15 NA) laser with a pair of FBGs, which emitted a maximum power of 10 W. The mode-matching of each pump was designed individually for efficient coupling. The two pump sources were combined together by a dichroic mirror (DM) M_1 and then focused into the Er:ZBLAN fiber by an anti-reflectively coated ZnSe aspheric lens ($f = 12.7$ mm, Edmund #64-124). The generated mid-infrared laser was separated from pump beams by coated mirror M_2.

Figure 2 shows the absorption of pump light at 1973 nm versus launched pump power of 970 nm. We measured the fiber transmission of 1973 nm pump light to be ~76% without the 970 nm pump. As the launched pump light at 970 nm increases, more electrons in the ground state are excited to the "virtual ground state"; thus, the absorption of pump light at 1973 nm becomes stronger, and residual pump power at 1973 nm remarkably decreases. In order to measure the residual pump power of 1973 nm, we filtered the 970 nm pump power with a same DM as M_1. Figure 2 shows that the residual 1973 nm pump power is ~7%. The residual pump light of 1973 nm may be attibuted to a small part of pump light coupled into the fiber cladding. In the experiment, we found that if the pump light was coupled into fiber cladding (remove the pump focal spot from fiber core), the absoprtion of pump light at 1973 nm would sharply decrease. According to the residual pump power of 1973 nm, we estimated that 93% of the 1973 nm pump was coupled into the fiber core.

Because the OC had a reflectivity of 40% at 2.8 μm, the Er:ZBLAN fiber laser emitted the 2.8 μm laser, while only the 970 nm pump light was employed. When we adopted the two pump lights of 970 and 1973 nm and increased the pump power of 1973 nm, the 2.8 μm laser emission gradually weakened and eventually disappeared. In order to measure the output power beyond 3.5 μm, we filtered the 2.8 μm laser with a DM before the power meter. Output powers of the Er:ZBLAN fiber laser as a function of the 1973 nm pump power are shown in Fig. 3 under different launched pump powers at 970 nm. Under the pump power of 1.16 W at 970 nm, the output power roll-over was observed as the launched pump power of 1973 nm

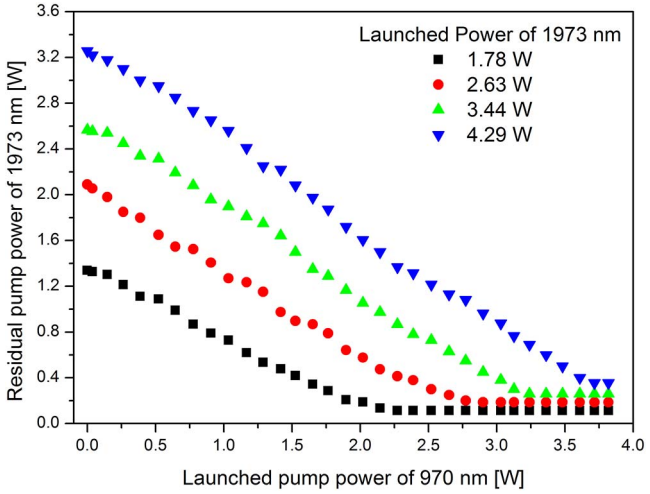

Fig. 2. (Color online) Residual pump power of 1973 nm as a function of 970 nm launched pump power for different launched powers at 1973 nm.

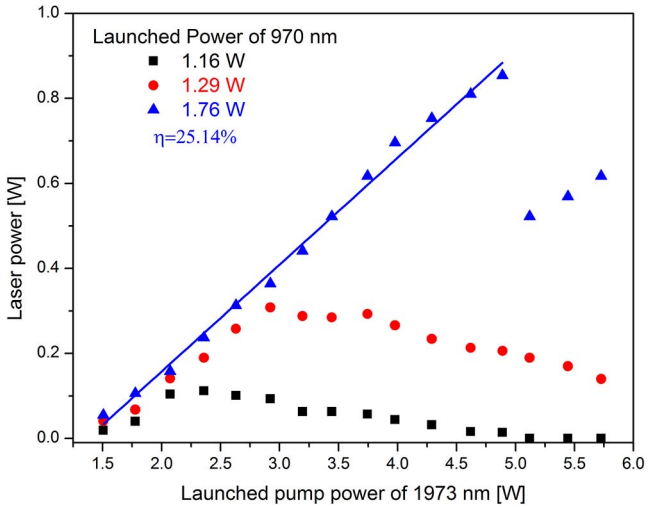

Fig. 3. (Color online) Output power as a function of the launched pump power at 1973 nm for different 970 nm pump powers of 1.16, 1.29, and 1.76 W, respectively.

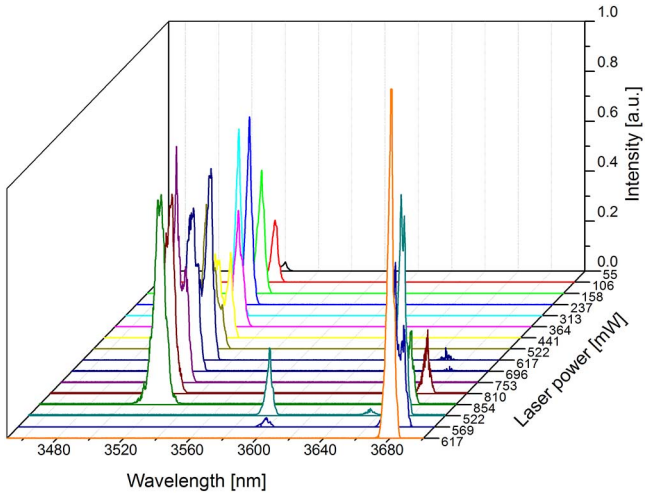

Fig. 4. (Color online) Laser spectrum evolution with output power.

was beyond 2.4 W. By slightly improving the pump power of 970 nm to 1.29 W, we could significantly delay the arrival of the power roll-over. This power roll-over phenomenon originates from the excited state absorption (ESA) of 1973 nm, which results in the population decrease of the upper laser level[26]. This problem can be overcome by increasing the pump power at 970 nm, which increases the population of the "virtual ground state" and makes more 1973 nm pump light be absorbed, thus, the ESA of 1973 nm becomes weak. When the pump power at 970 nm was set to 1.76 W, the laser output power increased linearly with a slope efficiency of 25.14% with respect to the 1973 nm pump light, and, finally, a maximum output power of 0.85 W was obtained under the 1973 nm pump power of 4.89 W. For the maximum output power of 0.85 W, the optical-to-optical efficiency was 12.72%. When the pump power at 1973 nm was beyond 4.89 W, a sharp decrease of output power was observed in the experiment. Meanwhile, we found the laser wavelength switched from 3.52 to 3.68 μm at this pump power, as shown in Fig. 4. The wavelength switching might be attributed to the excess population of the lower laser sublevel of $^4I_{9/2}$ that is not emptied fast enough in high-power operation, thus longer-wavelength lasing will arise by transiting to higher sublevel of $^4I_{9/2}$. According to the gain spectrum of Er:ZBLAN and the wavelength tuning result[23,24], the gain at 3.68 μm is significantly lower than that at 3.52 μm, which explains the reason why the output power has a dramatical drop after wavelength switching from 3.52 to 3.68 μm in our laser. Compared with the previous reports on 3.44–3.48, 3.55, and 3.60 μm operation of Er:ZBLAN fiber lasers[17–21,25], here, we report two new operation wavelengths at 3.52 and 3.68 μm in the Er:ZBLAN fiber laser. The operation wavelength of the laser could be switched by changing the launched pump power of 1973 nm. Under the low pump power of 1973 nm, the Er:ZBLAN fiber laser operated near 3520 nm with a bandwidth of ~5 nm and switched to 3680 nm with a bandwidth of ~4 nm beyond the pump power of 4.89 W. In order to protect the fiber facet from damage, we did not further increase the launched pump power. In order to observe the time-domain characteristics of the Er:ZBLAN fiber laser, we monitered the output laser with a mid-infrared photodetector (VIGO system, PCI-9) and a digital oscillator. No self-pulsing phonomenon was observed in the total pump power range.

We measured the beam quality of the output laser with the knife-edge method, as shown in Fig. 5. The measured M^2 value was 1.01, indicating that the laser output beam was diffraction-limited. We also captured the output beam profile with a thermosensitive card (VRC6S, Thorlabs). The inset of Fig. 5 shows that the laser beam has a round beam profile.

In order to test the power stability of the Er:ZBLAN fiber laser, we monitored the output power fluctuation

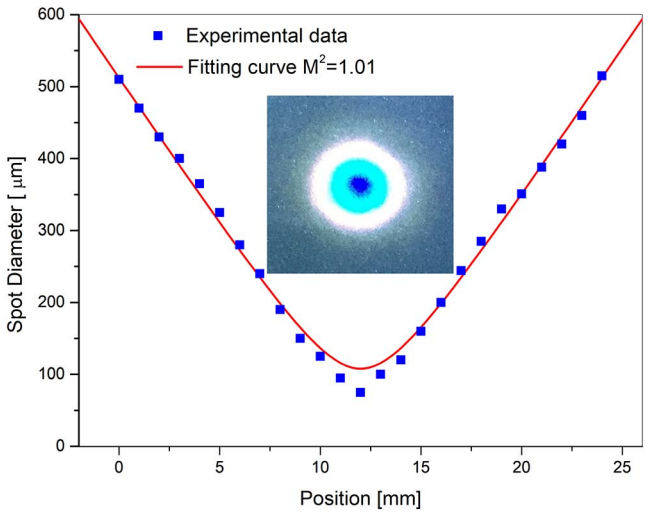

Fig. 5. Measurement of laser beam quality. Inset: beam profile.

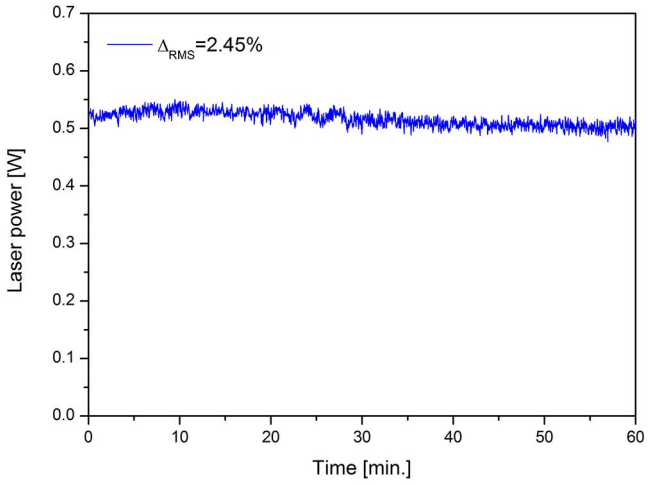

Fig. 6. Power stability of the Er:ZBLAN fiber laser.

for an hour at the launched 1973 nm pump power of 3.5 W, as shown in Fig. 6. The output power fluctuation (Δ_{RMS}) is ~2.45%. The slight power fluctuation could be attributed to the mechanical vibration of the pump source and Er:ZBLAN fiber, which will change the coupling efficiency between the 1973 nm pump light and the Er:ZBLAN fiber. Besides, mechanical vibration of the bulk reflectors also had an influence on the stability of the laser, since it changed the feedback of the laser. By splicing the fiber of the pump light and Er:ZBLAN fiber or substituting the bulk reflectors with FBGs, the power stability can be improved in the future[21,26].

In conclusion, we report on a mid-infrared Er:ZBLAN fiber laser reaching 3.68 μm wavelength based on the DWP scheme. The laser emission wavelength can be switched between 3.52 and 3.68 μm by changing the launched pump power at 1973 nm. The maximum output power of 0.85 W is obtained with a slope efficiency of 25.14% with respect to the 1973 nm pump power at 3.52 μm, and a significant power of 0.62 W is generated at 3.68 μm. To the best of our knowledge, the wavelength of 3.68 μm is the longest operation wavelength in free-running Er:ZBLAN fiber lasers so far.

This work was partially supported by the National Basic Research Program of China (No. 2013CBA01505), the Shanghai Excellent Academic Leader Project (No. 15XD1502100), the National Natural Science Foundation of China (No. 61675130), and the National Postdoctoral Program for Innovative Talents (No. 190375).

References

1. B. G. Lee, M. A. Belkin, R. Audet, J. MacArthur, L. Diehl, C. Pflügl, F. Capasso, D. C. Oakley, D. Chapman, A. Napoleone, D. Bour, S. Corzine, G. Höfler, and J. Faist, Appl. Phys. Lett. **91**, 231101 (2007).
2. H. H. P. Th. Bekman, J. C. van den Heuvel, F. J. M. van Putten, and H. M. A. Schleijpen, Proc. SPIE **5615**, 27 (2004).
3. D. Halmer, S. Thelen, P. Hering, and M. Mürtz, Appl. Phys. B **85**, 437 (2006).
4. J. J. Scherer, J. B. Paul, H. J. Jost, and M. L. Fischer, Appl. Phys. B **110**, 271 (2013).
5. Y. Shang, M. Shen, P. Wang, X. Li, and X. Xu, Chin. Opt. Lett. **14**, 121901 (2016).
6. M. Razeghi, N. Bandyopadhyay, Y. Bai, Q. Lu, and S. Slivken, Opt. Mater. Express **3**, 1872 (2013).
7. C. Yang, Y. Ju, B. Yao, Z. Zhang, T. Dai, and X. Duan, Chin. Opt. Lett. **14**, 061403 (2016).
8. V. Fortin, M. Bernier, S. T. Bah, and R. Vallée, Opt. Lett. **40**, 2882 (2015).
9. Y. O. Aydin, V. Fortin, F. Maes, F. Jobin, S. D. Jackson, R. Vallée, and M. Bernier, Optica **4**, 235 (2017).
10. S. Tokita, M. Murakami, S. Shimizu, M. Hashida, and S. Sakabe, Opt. Lett. **36**, 2812 (2011).
11. Z. Qin, G. Xie, H. Zhang, C. Zhao, P. Yuan, S. Wen, and L. Qian, Opt. Express **23**, 24713 (2015).
12. C. Wei, H. Luo, H. Zhang, C. Li, J. Xie, J. Li, and Y. Liu, Laser Phys. Lett. **13**, 105108 (2016).
13. P. Tang, Z. Qin, J. Liu, C. Zhao, G. Xie, S. Wen, and L. Qian, Opt. Lett. **40**, 4855 (2015).
14. Z. Qin, G. Xie, G. Zhao, S. Wen, P. Yuan, and L. Qian, Opt. Lett. **41**, 56 (2016).
15. S. Duval, M. Bernier, V. Fortin, J. Genest, M. Piché, and R. Vallée, Optica **2**, 623 (2015).
16. S. Antipov, D. D. Hudson, A. Fuerbach, and S. D. Jackson, Optica **3**, 1373 (2016).
17. H. Többen, Frequenz **45**, 250 (1991).
18. H. Többen, Electron. Lett. **28**, 1361 (1992).
19. O. Hendeson-Sapir, D. Ottaway, and J. Munch, in *Frontiers in Optics* (Optical Society of America, 2013), paper FW4B.1.
20. O. Henderson-Sapir, J. Munch, and D. J. Ottaway, Opt. Lett. **39**, 493 (2014).
21. F. Maes, V. Fortin, M. Bernier, and R. Vallée, Opt. Lett. **42**, 2054 (2017).
22. Y. D. Huang, M. Mortier, and F. Auzel, Opt. Mater. **17**, 501 (2001).
23. O. Henderson-Sapir, A. Malouf, N. Bawden, J. Munch, S. D. Jackson, and D. J. Ottaway, IEEE J. Sel. Top. Quantum Electron. **23**, 0900509 (2017).
24. O. Henderson-Sapir, S. D. Jackson, and D. J. Ottaway, Opt. Lett. **41**, 1676 (2016).
25. F. Maes, V. Fortin, M. Bernier, and R. Vallée, IEEE J. Quantum Electron. **53**, 1600208 (2017).
26. H. Okamoto, K. Kasuga, and Y. Kubota, Opt. Lett. **36**, 1470 (2011).